East European Journal of Physics. 1. 276-283 (2025)
DOI:10.26565/2312-4334-2025-1-32 ISSN 2312-4334

DOPING OF SILICON WITH GADOLINIUM ATOMS – STRUCTURAL DISTRIBUTION AND RAMAN SPECTRAL CHANGES

Sh.B. Utamuradova[a], Sh.Kh. Daliev[a], J.J. Khamdamov[a], Kh.J. Matchonov[a]*, M.K. Karimov[b], Kh.Y. Utemuratova[c]

[a]*Institute of Semiconductor Physics and Microelectronics at the National University of Uzbekistan, 20 Yangi Almazar st.,*
[b]*Urgench State University, Department of Physics, Urgench, Uzbekistan*
[c]*Karakalpak State University, Nukus, Karakalpakstan*
**Corresponding Author e-mail: husniddin94_04@bk.ru*
Received October 17, 2024; revised February 6, 2025; in final form February 10, 2025; accepted February 11, 2025

In this study, we investigated silicon samples doped with gadolinium using two different methods: incorporation during growth and diffusion treatment at elevated temperatures. Scanning electron microscopy (SEM) and energy-dispersive spectroscopy (EDS) were used to analyze the surface microstructure and impurity atom distribution, while Raman spectroscopy revealed characteristic phonon mode shifts induced by gadolinium doping. It was found that doping during growth results in a more uniform structure with fewer large defects, although localized regions enriched in carbon and oxygen remain. In contrast, diffusion doping leads to the formation of pronounced inhomogeneities, indicating significant dislocation formation and structural defects due to lattice parameter mismatches. The results demonstrate the influence of the doping method on the silicon surface state, elastic stress distribution, and the emergence of new vibrational modes, which can be utilized for the targeted modification of material properties in spintronic, optoelectronic, and sensor devices.
Keywords: *Silicon; Gadolinium; Doping; Diffusion; SEM; EDS; Raman Spectroscopy; Structural defects; Phonon Spectra; Crystal Lattice Defects; Optoelectronics; Magnetic Characteristics*
PACS: 68.37.Hk, 33.20.Fb

INTRODUCTION

Silicon is a key material in the modern semiconductor and optoelectronic industries due to its unique electrical and optical properties [1–6]. However, to expand its scope of application, its characteristics require modification. One promising approach to such modification is the introduction of rare earth elements, in particular gadolinium (Gd), which can significantly affect the magnetic and optical properties of silicon. Studies show that the integration of gadolinium atoms into the silicon crystal lattice changes its interaction with light and magnetic characteristics, which opens up new prospects for the use of such materials in optoelectronics, sensor devices, and spintronics.

Doping silicon with gadolinium atoms leads to structural changes that significantly affect its optical and magnetic properties. In particular, the introduction of Gd causes deformations of the crystal lattice and changes the optical activity of silicon. According to a number of studies, the inclusion of gadolinium can increase the photochemical (photoactive) ability of silicon to interact with radiation. This is explained by the fact that gadolinium retains localized f-electrons and, hence, magnetic moments even when embedded in a silicon lattice, which is especially important for spintronic applications [5–11].

One of the key effects of gadolinium doping in silicon is the reduction in the density of dangling bonds. It has been established that trivalent Gd^{3+} ions contribute to minimizing defects in the crystal structure, thereby improving the electronic properties of the material and reducing the number of surface imperfections. Additionally, gadolinium interacts with silicon to enhance the magnetic properties of the system, making it more suitable for applications in magnetic sensors and spintronic devices.

Despite these beneficial effects, certain limitations arise when doping silicon with gadolinium. Firstly, the distribution of Gd within the crystal volume can be uneven, making it challenging to achieve reproducible material characteristics-an issue particularly critical for high-precision devices. Secondly, localized stresses and defects introduced into the crystal lattice may restrict the efficiency of silicon in specific applications, such as photonic devices and high-frequency microelectronics.

Raman spectroscopy (RS) is an effective method for studying crystalline materials, including semiconductors such as silicon [12-15]. During the Raman scattering process, light interacts with phonons (quanta of crystal lattice vibrations), leading to changes in the energy and frequency of the scattered photons and the formation of characteristic spectral lines. Analyzing these spectral changes allows for the identification of structural defects and material properties.

Doping silicon with rare-earth elements such as gadolinium significantly influences the defect structure and deformation processes within the crystal lattice. The corresponding changes in Raman spectra reflect these structural rearrangements, providing insights into the nature of the defects that emerge. Understanding how the incorporation of Gd alters Raman scattering in silicon is of great interest for practical applications in electronics, optics, and nanotechnology. This study focuses on the analysis of one- and two-phonon Raman spectra of single-crystal silicon doped with gadolinium atoms.

Cite as: Sh.B. Utamuradova, Sh.Kh. Daliev, J.J. Khamdamov, Kh.J. Matchonov, M.K. Karimov, Kh.Y. Utemuratova, East Eur. J. Phys. 1, 276 (2025), https://doi.org/10.26565/2312-4334-2025-1-32

MATERIALS AND METHODS

For the investigation, n-Si and p-Si samples with an initial resistivity of 0.3–40 Ω·cm were prepared. Prior to doping, the samples underwent thorough acid-peroxide cleaning, followed by the removal of oxide layers using an HF solution. High-purity gadolinium films (99.999%) were deposited onto the cleaned silicon surfaces via vacuum deposition under high-vacuum conditions (10^{-7}–10^{-8} Torr). Doping was carried out through diffusion at 1473 K for 20 hours, followed by rapid cooling. The structural and elemental characteristics of the resulting materials were analyzed using energy-dispersive spectroscopy (EDS) and scanning electron microscopy (SEM).

RESULTS AND DISCUSSION

A visual analysis of the microscopic images in Fig. 1a reveals that the distribution of carbon (C) and silicon (Si) atoms on the sample surface is non-uniform. The carbon distribution map shown in Fig. 1b highlights areas of localized carbon accumulation, which may result from surface effects and the interaction of carbon with lattice defects.

The energy-dispersive spectroscopy (EDS) spectra presented in Fig. 2 confirm that silicon is the predominant element in the sample composition, as indicated by the intensity of its main peak. The presence of low-intensity oxygen (O) and carbon (C) peaks suggests the formation of oxide compounds or surface contamination, which may have occurred during sample growth or storage. The quantitative analysis summarized in Table 1 shows that the weight fraction of silicon is 86.79%, carbon 11.90%, and oxygen 1.96%. The high atomic concentration of carbon (23.81%) indicates its significant presence in the surface layer.

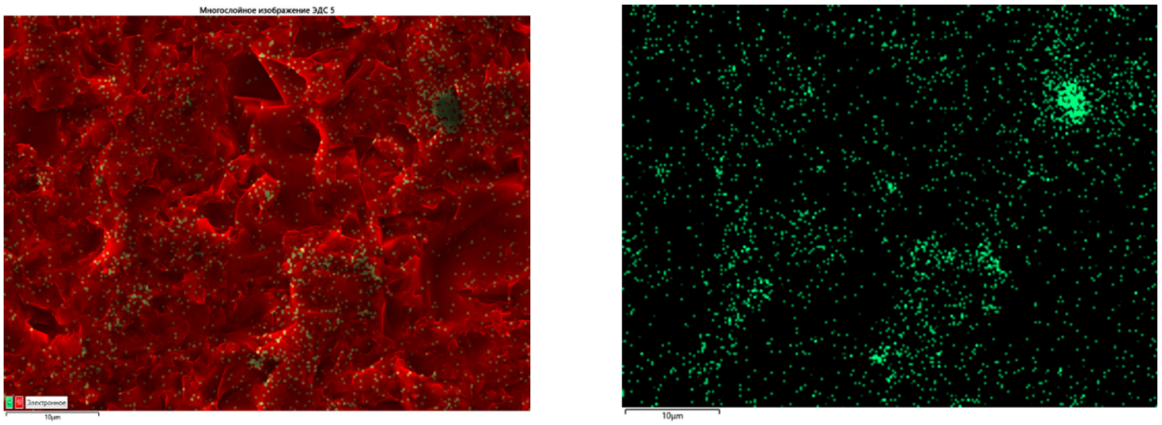

a) **b)**

Figure 1. SEM images of the surface of silicon doped with gadolinium during growth: (a) elemental distribution; (b) carbon distribution map.

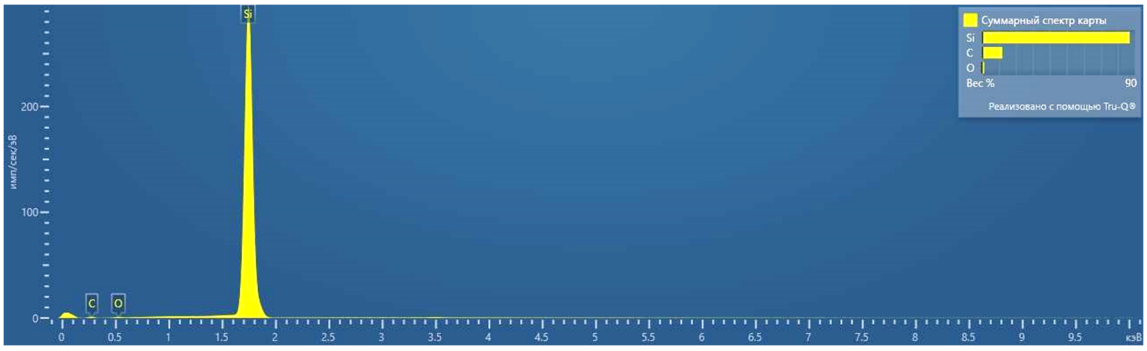

Figure 2. SEM spectrum of silicon doped with gadolinium during growth.

Table 1. Summary of elemental distribution maps for silicon doped with gadolinium during growth.

Element	Line Type	Conditional Concentration	Wt %	At. %
C (Carbon)	K-series	0.61	11.90	23.81
O (Oxygen)	K-series	0.56	1.31	1.96
Si (Silicon)	K-series	92.59	86.79	74.23
Total:			100.00	100.00

After heat treatment at 1473 K for 20 hours, the microstructure of the sample undergoes significant changes, as seen in Fig. 3. In the doped sample (Fig. 3b), compared to the original silicon (Fig. 3a), pronounced surface heterogeneity is observed. This may be attributed to the formation of defective regions, phase inclusions, and the redistribution of elements within the crystal lattice.

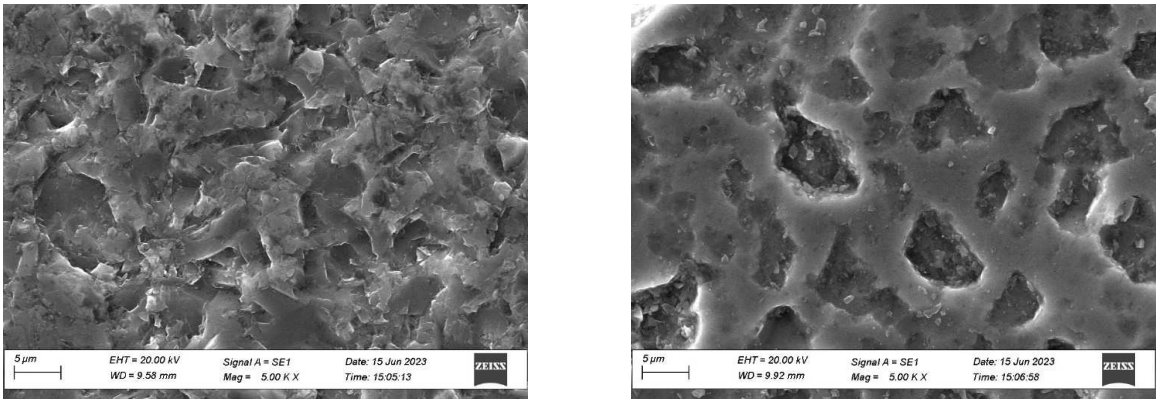

a) **b)**

Figure 3. SEM images of silicon: (a) original sample; (b) silicon doped with gadolinium via diffusion at 1473 K for 20 hours, illustrating microstructural changes in the material.

The results of energy-dispersive analysis after diffusion doping, presented in Fig. 4 and Table 2, indicate an increase in carbon content to 14.27% and a decrease in oxygen concentration to 1.20%. This change may be attributed to the selective sorption of carbon in regions with structural defects.

Figure 4. SEM spectrum of silicon doped with gadolinium via diffusion at 1473 K for 20 hours, illustrating microstructural changes in the material

Table 2. Summary of elemental distribution maps for silicon doped with gadolinium via the diffusion method at 1473 K for 20 hours.

Element	Line Type	Conditional Concentration	Wt %	At. %
C (Carbon)	K-series	0.61	11.90	23.81
O (Oxygen)	K-series	0.56	1.31	1.96
Si (Silicon)	K-series	92.59	86.79	74.23
Total:			100.00	100.00

A visual analysis of the microscopic images in Fig. 5 reveals that the diffusion of gadolinium into silicon results in large defect zones, as well as areas with pronounced porosity or a disordered structure. These structural inhomogeneities may be attributed to the following factors:

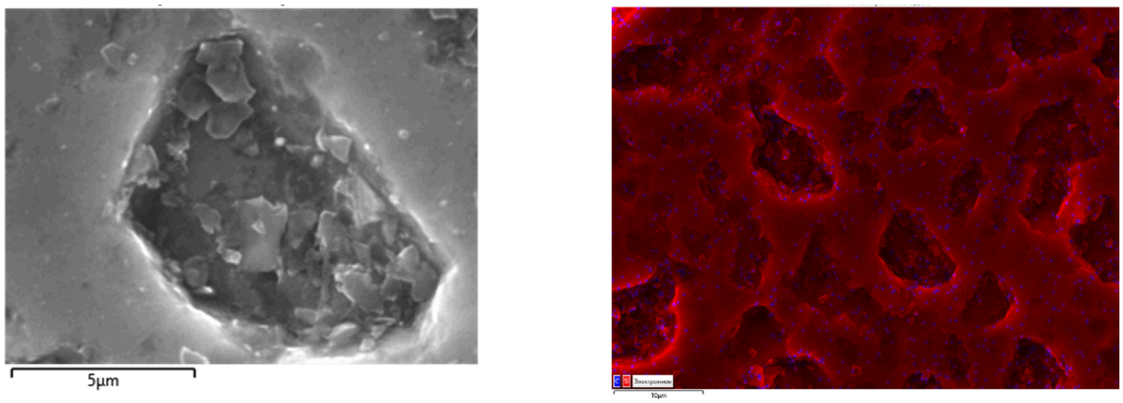

a) **b)**

Figure 5. SEM images of silicon doped with gadolinium via the diffusion method at 1473 K for 20 hours, illustrating defect formation and structural changes in the material.

Crystal lattice deformations – The incorporation of gadolinium introduces additional stress centers, leading to localized distortions in the silicon structure.

Phase transitions – The formation of new phases or solid solutions based on Gd–Si results in a non-uniform distribution of gadolinium atoms, causing localized chemical and structural changes.

Surface effects and contamination – The increased presence of carbon (C) and oxygen (O) may indicate surface oxidation or the trapping of these elements in defect regions. This effect is particularly common during high-temperature processing and subsequent cooling.

A comparison of microstructural changes and chemical composition reveals that diffusion doping with gadolinium significantly alters the surface layer of silicon. This process promotes the formation of large defects, including pores, potential cracks, and localized zones of gadolinium concentration with impurities. The energy-dispersive spectra of defect zones, presented in Fig. 6 and Table 3, confirm a decrease in oxygen content (0.73%) while maintaining an elevated carbon concentration (13.15%). This observation suggests variations in the sorption mechanisms of impurity elements within defect regions.

Figure 6. SEM spectrum of elemental distribution in defect regions of silicon doped with gadolinium via diffusion at 1473 K for 20 hours, illustrating microstructural changes in the material.

Table 3. Summary of elemental distribution maps in defect regions of silicon doped with gadolinium via the diffusion method at 1473 K for 20 hours.

Element	Line Type	Conditional Concentration	Wt %	At. %
C (Carbon)	K-series	0.65	13.15	26.02
O (Oxygen)	K-series	0.29	0.73	1.08
Si (Silicon)	K-series	87.12	86.13	72.90
Total:			100.00	100.00

Diffusion doping with gadolinium at 1473 K for 20 hours results in pronounced microstructural heterogeneity, characterized by the formation of defective regions, elemental redistribution, and localized phase transformations. In the doped samples, an increase in carbon concentration to 14.27% is observed, likely due to its selective sorption at structural defects. In defective zones, a reduced oxygen content (0.73%) is recorded, which is probably related to differences in the adsorption kinetics of oxygen and carbon.

Raman scattering (RS) analysis of gadolinium-doped silicon samples was performed using a SENTERRA II Raman spectrometer (Bruker), which offers high spectral sensitivity and a resolution of approximately 4.0 cm^{-1}. To ensure measurement accuracy (~0.2 cm^{-1}), automatic calibration was conducted using NIST standards (acetaminophen, silicon).

The spectra were excited using a 532 nm laser with a maximum power of 25 mW. Spectral data were recorded in the range of 50-4265 cm^{-1}, with an exposure time of 100 s, followed by summation of two spectra. To ensure accurate intensity comparisons between samples, the spectra were normalized to the peak at 510 cm^{-1}, which is the most intense in the analyzed range. Prior to normalization, the baseline was subtracted from each spectrum.

According to the literature [12-18], the lattice constant mismatch between Gd and Si can induce significant elastic stresses in thin layers, affecting both the electronic band structure and phonon spectra. Additionally, when there is a large discrepancy between lattice parameters in epitaxial multilayer structures, numerous defects are formed, degrading the quality of heterostructures. In the case of a Gd_xSi_{1-x} solid solution, lattice deformation is less critical compared to pure components (Gd and Si), as the actual lattice constant of the Gd_xSi_{1-x} layer lies between the values for Gd and Si. Furthermore, the layer thickness (5 μm) facilitates stress relaxation. Changes in the vibrational (phonon) spectra in this system clearly indicate the presence of Gd–Si bonds.

Doping silicon with gadolinium induces significant modifications in its vibrational spectra. These alterations stem from the incompatibility between the lattice parameters of Gd and Si, leading to the formation of structural defects and localized mechanical stresses.

Fig. 7 presents the Raman spectrum of gadolinium-doped p-type silicon with a resistivity of 0.3 Ω·cm. Spectrum analysis reveals a significant broadening of the main peak at 510 cm^{-1}, indicating an increased density of defects in the

crystal lattice. Additionally, extra vibrational modes are observed at 123, 148, 238, and 303 cm^{-1}, which may be attributed to the formation of impurity complexes and localized structural distortions.

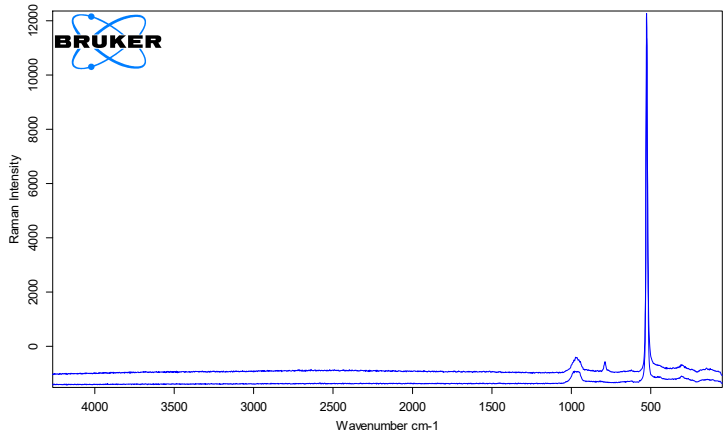

Figure 7. Raman spectrum of p-type silicon doped with gadolinium (Gd):
1 – Raman spectrum of the initial Si samples; 2 – Raman spectrum of p-Si<Gd> samples with an initial resistivity of ρ = 0.3 Ω·cm.

Fig. 8 presents the Raman spectra of n-type silicon samples with a specific resistivity of 10 Ω·cm.

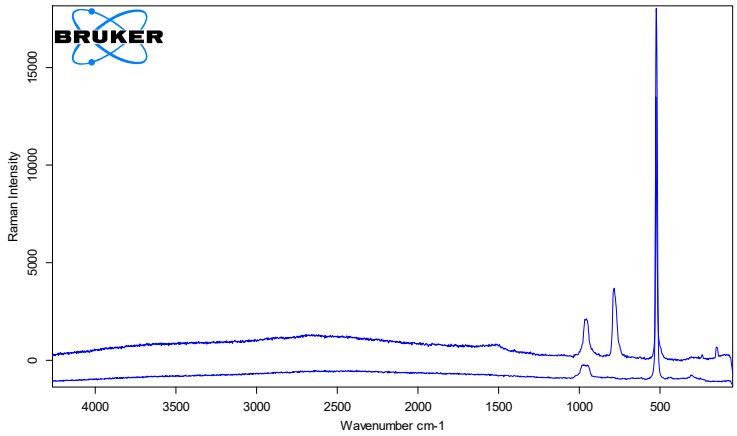

Figure 8. Raman spectrum of n-type silicon doped with gadolinium (Gd):
1 – Raman spectrum of the initial Si samples; 2 – Raman spectrum of n-Si<Gd> samples with an initial resistivity of ρ = 10 Ω·cm.

With increasing specific resistivity, an enhancement in the intensity of additional spectral lines is observed, indicating modifications in the band structure of silicon due to the incorporation of gadolinium atoms. In particular, the intensification of the bands at 456 cm^{-1} and 954 cm^{-1} may be associated with the formation of amorphous phases and the presence of oxide inclusions.

Fig. 9 presents the Raman spectra of n-type silicon samples with a specific resistivity of 15 Ω·cm.

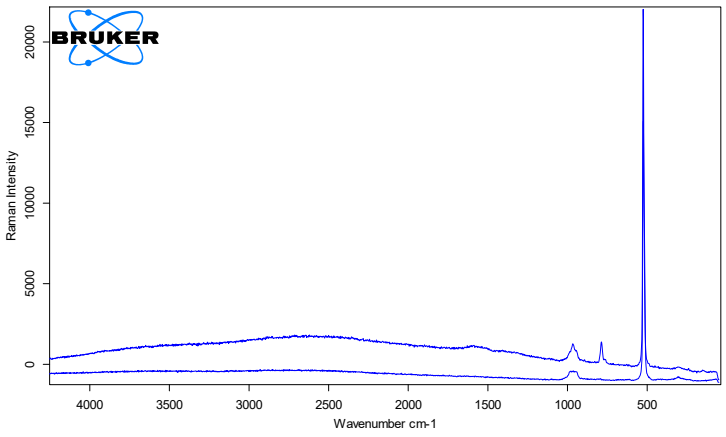

Figure 9. Raman spectrum of n-type silicon doped with gadolinium (Gd):
1 – Raman spectrum of the initial Si samples; 2 – Raman spectrum of Gd_xSi_{1-x} samples with an initial resistivity of ρ = 15 Ω·cm.

This spectrum exhibits a further enhancement of vibrational modes in the region of 68, 784, 1340, and 1610 cm^{-1}, which may be attributed to the formation of stable Gd–Si impurity complexes. Of particular interest is the intense peak at 784 cm^{-1}, which can be interpreted as evidence of a strong chemical bond between gadolinium and silicon atoms.

Solid solutions of Gd–Si with varying Gd and Si content are characterized by frequency shifts in the local vibrations of Gd–Gd, Gd–Si, and Si–Si, associated with variations in strain within the films. According to Raman spectroscopy data, three primary vibrational regions can be identified [14-20]: Gd–Gd near 238 cm^{-1}, Gd–Si around 783 cm^{-1}, Si–Si at approximately 510 cm^{-1}.

The position of these spectral lines is significantly influenced by built-in stresses resulting from the considerable lattice parameter mismatch between Gd and Si [18-25 It is well known that during epitaxial growth of a layer on a substrate with a different lattice constant, an initial pseudomorphic layer forms, adapting to the substrate. However, once a critical thickness is reached, the formation of dislocations becomes energetically favorable, after which the layer grows with its own lattice constant. Such layers are referred to as relaxed or unstressed layers [18].

The frequency shift of the optical phonon mode in the crystal can also be described by the Grüneisen parameter [12], which relates the change in unit cell volume to the shift in optical phonon frequencies. This shift is presumed to result from hydrostatic (isotropic) compression or expansion of the unit cell due to the incorporation of Gd atoms.

In the region of 521–522 cm^{-1}, an intense peak is observed, corresponding to first-order scattering of optical phonons (TO – transverse optical vibrations, LO – longitudinal optical vibrations) at the Γ point of the Brillouin zone. Additionally, a detailed analysis of the peaks near 123 and 186 cm^{-1}, using Gaussian approximation, allows them to be associated with the vibrational modes of Gd [17]. The mode at 148 cm^{-1} is related to first-order scattering of acoustic phonons (TA – transverse acoustic vibrations), which may reflect vibrational contributions from the oxide film (SiO_2). The weak-intensity LO peak at 456 cm^{-1} suggests the presence of amorphous silicon components [18].

The second-order spectrum is significantly weaker, appearing in the range of approximately 100-1100 cm^{-1}. The peak around 303 cm^{-1} is typically attributed to 2TA acoustic phonons, while the broad signal between 900 and 1000 cm^{-1} is associated with 2TO phonons [12]. Furthermore, the broadening of specific peaks (e.g., in the regions of 68, 954, 1340, and 1610 cm^{-1}) suggests a high defect density or compositional fluctuations [19].

A comparison with literature sources indicates that the modes near 954, 1340, and 1610 cm^{-1} correspond to GdO vibrations, while the peaks at 1462 and 1600 cm^{-1} may be associated with third-order Raman modes related to silicon optical phonons (TO) and interstitial oxygen (O_2) vibrations, respectively [17–26].

Fig. 10 presents the Raman spectra of samples with a specific resistivity of 40 Ω·cm.

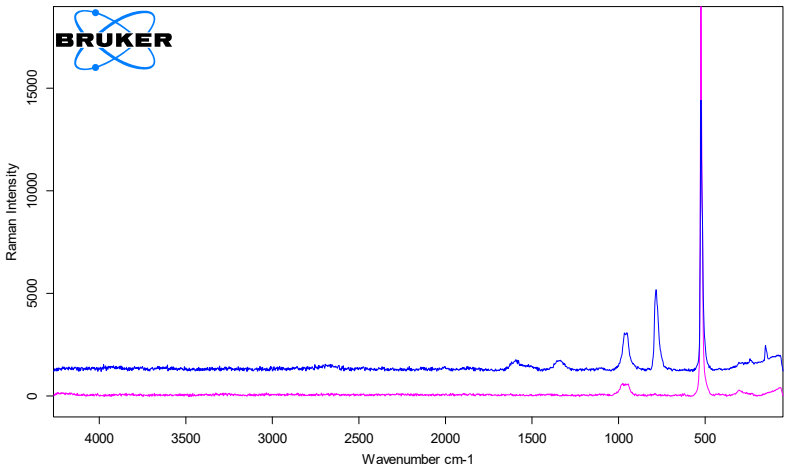

Figure 10. Raman spectrum of n-type silicon doped with gadolinium (Gd):
1 – Raman spectrum of the initial Si samples; 2 – Raman spectrum of Gd_xSi_{1-x} samples with an initial resistivity of ρ = 40 Ω·cm.

With a further increase in specific resistivity, a significant enhancement of spectral lines in the 784 - 1610 cm^{-1} range is observed, indicating a redistribution of local stresses within the crystal lattice and the formation of band engineering effects. The presence of characteristic vibrational modes Gd–Gd (~238 cm^{-1}), Gd–Si (~783 cm^{-1}), and Si–Si (~510 cm^{-1}) confirms the incorporation of gadolinium into the silicon lattice and its influence on the material's structure.

A comparative analysis of Raman spectra for samples with different initial resistivities (0.3, 13, 15, and 40 Ω·cm) reveals that with increasing resistivity - and consequently, higher Gd concentration—the intensity of peaks at ~68, 123, 148, 238, 303, 456, 784, 954, 1340, and 1610 cm^{-1} increases. The most intense peak at ~784 cm^{-1} is likely associated with Gd–Si bond vibrations.

A comparison of the results obtained from two different gadolinium doping methods—during growth and diffusion at 1473 K - demonstrates significant differences in alloying element distribution and defect formation. In the case of doping during growth, SEM images indicate a more uniform incorporation of Gd, with relatively fewer large structural defects. However, localized impurity clusters (C, O) are present, which may reflect process-specific characteristics such as incomplete surface cleaning or oxidation.

In contrast, diffusion doping at high temperatures results in more pronounced microstructural inhomogeneities and the formation of large defect zones (pores, cracks), caused by a significant lattice parameter mismatch between Gd and Si and intense dislocation formation. However, this method facilitates stress relaxation in thicker layers, as confirmed by phonon mode shifts in Raman spectra and the emergence of spectral lines associated with Gd–Si bonds.

Thus, doping during growth is preferable when thin, uniform layers with minimal large defects are required, whereas diffusion doping allows for greater control over composition and thickness but is associated with a higher density of structural defects.

The observed Raman spectral changes in gadolinium-doped silicon samples confirm the formation of Gd–Si bonds and structural modifications induced by Gd incorporation. Given that Gd doping introduces elastic stresses and localized defects, these findings provide a foundation for further optimization of processing techniques to develop functional materials with tailored electrical and optoelectronic properties.

A comparative analysis of the obtained data highlights the significant impact of doping mechanisms on the material's spectral characteristics:

Sputtering followed by crystallization ensures a uniform gadolinium distribution but is accompanied by localized oxygen and carbon accumulations, likely due to surface oxidation.

Diffusion doping at 1473 K results in intensive dislocation formation, pore generation, and point defects due to Gd-Si lattice incompatibility. However, stress relaxation occurs, as evidenced by spectral shifts in vibrational modes.

Therefore, the sputtering method with subsequent crystallization produces structurally homogeneous layers, whereas diffusion doping enables precise control over composition and thickness but is accompanied by more pronounced crystallographic rearrangements.

CONCLUSIONS

The analysis of Raman spectra in gadolinium-doped silicon confirms the significant influence of impurity atoms on the material's vibrational characteristics. New spectral modes at 68, 123, 148, 238, 303, 456, 784, 954, 1340, and 1610 cm^{-1} are observed, with their intensity increasing as the Gd concentration rises.

The formation of strong Gd–Si bonds is confirmed by the presence of a characteristic vibrational line at ~784 cm^{-1}. The results indicate that the defect structure plays a crucial role in the redistribution of impurity atoms, thereby altering the electrical, optical, and magnetic properties of doped silicon.

A comparative analysis demonstrates that gadolinium diffusion into silicon leads to the formation of complex defect-phase structures, which can either enhance material properties-such as promoting magnetic ordering-or degrade mechanical stability and electrical performance.

Optimizing diffusion parameters, including temperature, holding time, and cooling rate, is essential for achieving a balance between structural, chemical, and functional properties of gadolinium-doped silicon.

ORCID

Sharifa B. Utamuradova, https://orcid.org/0000-0002-1718-1122; **Jonibek J. Khamdamov**, https://orcid.org/0000-0003-2728-3832
Khusniddin J. Matchonov, https://orcid.org/0000-0002-8697-5591

REFERENCES

[1] S.B. Utamuradova, S.K. Daliev, A.K. Khaitbaev, J.J. Khamdamov, Kh.J. Matchonov, and X.Y. Utemuratova, "Research of the Impact of Silicon Doping with Holmium on its Structure and Properties Using Raman Scattering Spectroscopy Methods," East European Journal of Physics, (2), 274-278 (2024). https://doi.org/10.26565/2312-4334-2024-2-28

[2] J. Yang, Y. Feng, X. Xie, H. Wu, and Y. Liu, "Gadolinium-doped silicon clusters GdSin (n=2-9) and their anions: structures, thermochemistry, electron affinities, and magnetic moments", Theor Chem Acc, **135**, 204 (2016) https://doi.org/10.1007/s00214-016-1964-z

[3] M.K. Karimov, Kh.J. Matchonov, K.U. Otaboeva, and M.U. Otaboev, "Computer Simulation of Scattering Xe+ Ions from InP(001)⟨110⟩ Surface at Grazing Incidence," e-Journal of Surface Science and Nanotechnology, **17**, 179-183 (2019). https://doi.org/10.1380/ejssnt.2019.179

[4] M.S. Sercheli, amd C. Rettori, "Magnetic Properties of Gadolinium-Doped Amorphous Silicon Films," Brazilian Journal of Physics, **32**(2A), 409-411 (2002). https://doi.org/10.1590/S0103-97332002000200046

[5] M.K. Karimov, U.O. Kutliev, S.B. Bobojonova, and K.U. Otabaeva, "Investigation of Angular Spectrum of Scattered Inert Gas Ions from the InGaP (001) Surface," Physics and Chemistry of Solid State, **22**(4), 742–745 (2021). https://doi.org/10.15330/pcss.22.4.742-745

[6] Sh.B. Utamuradova, Kh.J. Matchonov, J.J. Khamdamov, and Kh.Y. Utemuratova, "X-ray diffraction study of the phase state of silicon single crystals doped with manganese". New Materials, Compounds and Applications, **7**(2), 93-99, (2023). http://jomardpublishing.com/UploadFiles/Files/journals/NMCA/v7n2/Utamuradova_et_al.pdf

[7] P.M. Fauchet, and I.H. Campbell, "Raman spectroscopy of low-dimensional semiconductors," Critical Reviews in Solid State and Materials Sciences, **14**(sup1), s79–s101 (1988). http://dx.doi.org/10.1080/10408438808244783

[8] S.B. Utamuradova, K.S. Daliev, A.I. Khaitbaev, J.J. Khamdamov, J.S. Zarifbayev, and B.S. Alikulov, "Defect Structure of Silicon Doped with Erbium," East European Journal of Physics, (2), 288-292 (2024) https://doi.org/10.26565/2312-4334-2024-2-31

[9] W. Yang, J. Chen, Y. Zhang, Y. Zhang, Jr.-H. He, and X. Fang, "Silicon-Compatible Photodetectors: Trends to Monolithically Integrate Photosensors with Chip Technology," Adv. Funct. Mater. **29**(18), 1808182 (2019). https://doi.org/10.1002/adfm.201808182

[10] M. Piels, and J.E. Bowers, "Photodetectors for silicon photonic integrated circuits," Photodetectors Materials, Devices and Applications, 3-20, (2016). https://doi.org/10.1016/B978-1-78242-445-1.00001-4

[11] K.S. Daliev, Sh.B. Utamuradova, J.J. Khamdamov, M.B. Bekmuratov, O.N. Yusupov, Sh.B. Norkulov, and Kh.J. Matchonov, "Defect Formation in MIS Structures Based on Silicon with an Impurity of Ytterbium," East Eur. J. Phys. (4), 301-304 (2024). https://doi.org/10.26565/2312-4334-2024-4-33
[12] Kh.S. Daliev, Sh.B. Utamuradova, Z.E. Bahronkulov, A.Kh. Khaitbaev, and J.J. Hamdamov, "Structure determination and defect analysis n-Si<Lu>, p-Si<Lu> by raman spectrometer methods," East Eur. J. Phys. (4), 193 (2023), https://doi.org/10.26565/2312-4334-2023-4-23
[13] R.R. Jones, D.C. Hooper, L. Zhang, D. Wolverson, and V.K. Valev, "Raman Techniques: Fundamentals and Frontiers," Nanoscale Research Letters, **14**(1), 231 (2019). https://doi.org/10.1186/s11671-019-3039-2
[14] U. Ramabadran, and B. Roughani, "Intensity analysis of polarized Raman spectra for off axis single crystal silicon," Materials Science and Engineering: B, **230**, 31–42 (2018). https://doi.org/10.1016/j.mseb.2017.12.040
[15] K.S. Daliev, Sh.B. Utamuradova, J.J. Khamdamov, Sh.B. Norkulov, and M.B. Bekmuratov, "Study of Defect Structure of Silicon Doped with Dysprosium Using X-Ray Phase Analysis and Raman Spectroscopy," East Eur. J. Phys. (4), 311-321 (2024). https://doi.org/10.26565/2312-4334-2024-4-35
[16] V.O. Vas'kovskiy, A.V. Svalov, A.V. Gorbunov, N.N. Schegoleva, and S.M. Zadvorkin, "Structure and magnetic properties of Gd/Si and Gd/Cu hybridization in lithium tetraborate," Frontiers in Physics, **2**, (2014). https://doi.org/10.3389/fphy.2014.00031
[17] K.S. Daliev, Sh.B. Utamuradova, J.J. Khamdamov, M.B. Bekmuratov, Sh.B. Norkulov, and U.M. Yuldoshev, "Changes in the Structure and Properties of Silicon During Ytterbium Doping: The Results of o Comprehensive Analysis," East Eur. J. Phys. (4), 240-249 (2024). https://doi.org/10.26565/2312-4334-2024-4-24
[18] K. Kasirajan, L.B. Chandrasekar, S. Maheswari, M. Karunakaran, and P.S. Sundaram, "A comparative study of different rare-earth (Gd, Nd, and Sm) metals doped ZnO thin films and its room temperature ammonia gas sensor activity: Synthesis, characterization, and investigation on the impact of dopant," Optical Materials, **121**, 111554 (2021). https://doi.org/10.1016/j.optmat.2021.111554
[19] T.D. Kelly, J.C. Petrosky, J.W. McClory, V.T. Adamiv, Y.V. Burak, B.V. Padlyak, I.M. Teslyuk, *et al*., "Rare earth dopant (Nd, Gd, Dy, and Er) hybridization in lithium tetraborate," Front. Phys. **2**, (2014). https://doi.org/10.3389/fphy.2014.00031
[20] A.I. Prostomolotov, Yu.B. Vasiliev, and A.N. Petlitsky, "Mechanics of defect formation during growth and heat treatment of single-crystal silicon," **4**(4), 1716–1718 (2011). http://www.unn.ru/pages/e-library/vestnik/19931778_2011_-_4-4_unicode/147.pdf
[21] S.Z. Zainabidinov, A.Y. Boboev, N.Y. Yunusaliyev, and J.N. Usmonov, "An optimized ultrasonic spray pyrolysis device for the production of metal oxide films and their morphology," East Eur. J. Phys. (3), 293 (2024), https://doi.org/10.26565/2312-4334-2024-3-30
[22] W.-E. Hong, and J.-S. Ro, "Kinetics of solid phase crystallization of amorphous silicon analyzed by Raman spectroscopy," J. Appl. Phys. **114**, 073511 (2013). https://doi.org/10.1063/1.4818949
[23] S. Zainabidinov, Sh.Kh. Yulchiev, A.Y. Boboev, B.D. Gulomov, and N.Y. Yunusaliyev, "Structural properties of Al-doped ZnO films," East Eur. J. Phys. (3), 282 (2024). https://doi.org/10.26565/2312-4334-2024-3-28
[24] R.T.-P. Lee, K.-M. Tan, T.-Y. Liow, C.-S. Ho, S. Tripathy, G.S. Samudra, D.-Z. Chi, and Y.-C. Yeo, "Probing the $ErSi_{1.7}$ Phase Formation by Micro-Raman Spectroscopy," Journal of The Electrochemical Society, **154**(5), H361-H364 (2007). https://doi.org/10.1149/1.2710201
[25] A.S. Zakirov, Sh.U. Yuldashev, H.J. Wang, H.D. Cho, T.W. Kang, J.J. Khamdamov, and A.T. Mamadalimov, "Photoluminescence study of the surface modified and MEH-PPV coated cotton fibers," Journal of Luminescence, 131(2), 301–305 (2011). https://doi.org/10.1016/j.jlumin.2010.10.019
[26] S. Zainabidinov, A.Y. Boboev, and N.Y. Yunusaliyev, "Effect of γ-irradiation on structure and electrophysical properties of S-doped ZnO films," East European Journal of Physics, (2), 321–326 (2024) https://doi.org/10.26565/2312-4334-2024-2-37

ЛЕГУВАННЯ КРЕМНІЮ АТОМАМИ ГАДОЛІНІЮ – СТРУКТУРНИЙ РОЗПОДІЛ ТА СПЕКТРАЛЬНІ ЗМІНИ КРЕМНІЮ

Ш.Б. Утамурадова[a], Ш.Х. Далієв[a], Д.Д. Хамдамов[a], Х.Д. Матчонов[a], М.К. Карімов[b], Х.Ю. Утемуратова[c]
[a]Інститут фізики напівпровідників і мікроелектроніки Національного університету Узбекистану, вул. Янги Алмазара, 20,
[b]Ургенчський державний університет, факультет фізики, Ургенч, Узбекистан
[c]Каракалпакський державний університет, Нукус, Каракалпакстан

У цьому дослідженні ми досліджували зразки кремнію, леговані гадолінієм, використовуючи два різні методи: включення під час росту та дифузійна обробка при підвищених температурах. Скануючу електронну мікроскопію (SEM) та енергодисперсійну спектроскопію (EDS) використовували для аналізу мікроструктури поверхні та розподілу атомів домішок, тоді як раманівська спектроскопія виявила характерні зсуви фононних мод, спричинені допуванням гадолінієм. Було виявлено, що легування під час росту призводить до більш однорідної структури з меншою кількістю великих дефектів, хоча локалізовані області, збагачені вуглецем і киснем, залишаються. Навпаки, дифузійне легування призводить до утворення виражених неоднорідностей, що вказує на значне утворення дислокацій і структурних дефектів через неузгодженість параметрів решітки. Результати демонструють вплив методу легування на стан поверхні кремнію, розподіл пружних напружень і появу нових коливальних мод, які можуть бути використані для цілеспрямованої модифікації властивостей матеріалів у спінтронних, оптоелектронних і сенсорних пристроях.

Ключові слова: *кремній; гадоліній; допінг; дифузія; SEM; EDS; Раманівська спектроскопія; структурні дефекти; фононний спектр; дефекти кристалічної решітки; оптоелектроніка; магнітні характеристики*